Assessing the nexus between groundwater and solar-energy plants in a desert basin with a dual-model approach under uncertainty

Kuai Fang[1], Xinye Ji, Chaopeng Shen[*,1], Noel Ludwig[2,†], Peter Godfrey[3†,], Tasnuva Mahjabin[1], and Christine Doughty[4]

[1] Civil and Environmental Engineering, Pennsylvania State University, University Park, PA
[2] Soil and Water Program Manager, Mt. Baker-Snoqualmie National Forest, US Department of Agriculture Forest Service, Everett WA
[3] Soil, Water, Air Program Lead, Wyoming State Office, Bureau of Land Management, US Department of Interior, Cheyenne, WY
[4] Earth and Environmental Sciences, Lawrence Berkeley National Laboratory, Berkeley CA

Abstract

Globally, many solar power plants and other types of renewable energy are being located in water-scarce regions. Many projects rely on groundwater resources whose sustainability is uncertain. In the Chuckwalla Basin in California, quantification of recharge and trans-valley underflow is needed to estimate the impacts of solar project withdrawals on the water table. However, such estimates are highly challenging due to data scarcity, heterogeneous soils and long residence times. Conventional assessment employs isolated groundwater models configured with crude and uniform estimates of recharge. Here, we employ a data-constrained surface-subsurface processes model, PAWS+CLM, to provide an ensemble of recharges and underflows with perturbed parameters. Then, the Parameter Estimation (PEST) package is used to calibrate MODFLOW aquifer conductivity and filter out implausible recharges. The novel dual-model approach, potentially applicable in other arid regions, can effectively assimilate groundwater head observations, reject unrealistic parameters, and narrow the range of estimated drawdowns. Simulated recharge concentrates along alluvial fans at the mountain fronts and ephemeral washes where run-off water infiltrates. If an evenly distributed recharge was assumed, it resulted in under-estimated drawdown and larger uncertainty bounds. The withdrawals are approaching total inflow, suggesting the system will be nearing, if not exceeding, its sustainable groundwater production capacity, and a boom of such projects will not be sustainable. Especially, the cost/benefit of pumped-storage projects is called into question as the initial-fill phase depletes entire area's recharge. Our study highlights the stress on groundwater resources of solar development, and that the speed of groundwater recovery does not indicate sustainability.

Main point 1: A novel dual model approach, involving an integrated surface/subsurface model and a groundwater parameter-estimation model, was able to better constrain the model.
Main point 2: The groundwater system may be nearing, if not exceeding, its sustainable groundwater production capacity and the speed of recovery is not indicative of sustainability.
Main point 3: Results from using conventionally-assumed uniform recharge distort calibrated K fields and impacts assessment

[*] Corresponding author: cshen@engr.psu.edu

[†] Work done at California Desert District, Bureau of Land Management

1. Introduction

On a global scale, many solar power plants and other renewable energy sources are being constructed in desert regions, e.g., the Sahara Desert (Jokadar and Ponte 2012), China's Gobi Desert (Alexandra Sims 2015), and Southern California, due to their abundance of sunlight and available space. This trend is expected to grow with the solar power industry. All types of solar plants require water for construction and operation, and the operation of concentrated solar power plants involves significantly more water for cooling and, potentially, energy storage. In many desert regions, groundwater is the only option to meet water demands, and the sustainability of groundwater emerges as an important question.

As a standout case, since 2008, a number of solar energy plants have been located in the Mojave and Sonoran Deserts, e.g., in California's Chuckwalla Basin, our study area (Figure 1). In addition, energy-storage projects (Rehman *et al.* 2015), e.g., the Eagle Mountain Pumped Storage (EMPS), are permitted to smooth the output to the grid by storing energy as potential energy. In the Chuckwalla, the approved solar plants collectively extract a total of 2.3 Mm^3yr^{-1} (1850 acre-ft/yr, or afy) from the local aquifer and the EMPS proposed to extract almost 10 Mm^3 yr^{-1} (8100 afy) during the 4-yr initial-fill phase (FERC 2012).

Because desert aquifers receive limited recharge, only limited groundwater can be renewably extracted. Estimating recharge in desert, mountainous basins is especially challenging because it occurs through spatially sporadic infiltration (Flint *et al* 2004) of ephemeral runoff along many washes descending from mountains (CADWR 1979) and through alluvial fans. Long-term collection of infiltration data in the many ephemeral washes is prohibitive and often unavailable. In addition, with water balance methods, small errors in evapotranspiration estimate results in large percentage error in recharge.

Conventionally, groundwater systems were often modeled in isolated groundwater models such as MODFLOW (Harbaugh 2005). In that paradigm, recharge needs to be estimated through independent means, e.g., as a percentage of precipitation (Maxey and Eakin 1949) or via precipitation-runoff regression (Wilson and Guan 2004, Scanlon 2004). Previous environmental impact assessments (EIAs) in the Chuckwalla Basin have used Maxey-Eakin-type estimate, assuming 2 to 10% of precipitation (WorleyParsons 2009, GEI 2010). However, this method has limitations as it does not consider location and mechanism of recharge (Maurer and Berger 2006) and. Physically-based integrated hydrologic models, e.g., GSFlow (Markstrom *et al* 2008, Tian *et al* 2015), HydroGeoSphere (Therrien *et al* 2006), ParFlow (Munévar and Mariño 1999), and PAWS (Shen and Phanikumar 2010), calculate recharge as an internal flux. Adapted properly for arid mountainous domains, they can serve as practical tools for recharge estimation.

Integrated hydrologic modeling also faces data scarcity. *First*, desert soil properties differ greatly from what could be inferred from pedotransfer functions (PTF) (Wösten *et al* 2001). For example, we find closely packed, interlocking rock fragments termed desert pavement (McFadden *et al* 1987) (Figure 2a). These soils are hydraulically distinct from soils elsewhere with similar sand/clay compositions and can vary substantially depending on age (Young *et al* 2004, Mirus *et al* 2009). Therefore, uncertainty analysis is necessary. *Second*, recharge can take decades to reach the deep water table, requiring non-trivial long-term simulations. *Finally*, aquifer conductivity (K) is poorly mapped. While there is some success in groundwater-model-only calibration using pilot points and regularization (Doherty 2003), no framework exists to heuristically utilize varied sources of information, e.g., groundwater head, soil moisture, and pumping test data, to constrain integrated modeling.

87 The overarching questions are whether modern recharge is sufficient to support proposed
88 groundwater production by solar plants and how the groundwater head will respond to that
89 production given large uncertainties. In this study, we devised an observationally-constrained
90 dual-model approach that combines a surface-subsurface process model with a groundwater flow
91 and parameter estimation package.

92 ## 2. Sites and Methods

93 ### 2.1. Basin physiographic properties

94 The Chuckwalla Basin (6712 km^2 or 2592 mi^2) is located west of the city of Blythe beside the
95 Colorado River in California (Figure 1), between the Mojave and Sonoran Deserts. The basin has
96 a hot desert climate, with average January and July temperatures of 4°C (39°F) and 43°C
97 (109°F), respectively, and an 18-year annual average rainfall of 95 mm (~3.5 inches). There are
98 no perennial water bodies within the basin. About 30% of the basin is mountainous terrain rising
99 abruptly from the valley floor. The floor slopes gently from northwest to southeast. It includes
100 the Pinto Valley in the northwest, as well as upper (western) and lower (eastern) portions of the
101 Chuckwalla Valley proper, with a subtle surface water divide between Palen and Ford Dry Lakes
102 (playas). The metamorphic and igneous bedrock composing the mountains is assumed to be
103 impervious (WorleyParsons 2009).

104 The mountains contain thin, sandy soils within washes and alluvial drainages. Valley surficial
105 materials include (i) coarse, steep alluvial fans at the mountain feet (Figure 2b); (ii) loamy sand
106 alluvium with interlacing desert pavement, and (iii) clay-rich playas near the center (USGS
107 1995). The SSURGO database contains only one soil type for most of the Chuckwalla Valley
108 and mountains, with no depth to bedrock, soil water retention, or conductivity data.

Well borehole logs indicate that the alluvial layer (interbedded sands and gravels with discontinuous clay) varies between 210 m (700 ft) and 366 m (1200 ft) in thickness (CADWR 1979). Depth to water table ranges from 150 m (485 ft) near Desert Center to 6.4 m (21 ft) near Palen Dry Lake, where groundwater may discharge slowly as evaporation. In the lower valley, underneath the alluvium is the productive Bouse Formation (Metzger *et al* 1973), a Pliocene marine and estuarine sequence composed of limestone, clay, silt, and sand (Owen-Joyce *et al* 2000). Well logs suggest its surface is flat (Stone 2006, WorleyParsons 2009). However, the Bouse is not noted west of Desert Center (GEI 2010). A Miocene Fanglomerate aquifer unconformably underlies the Bouse, but their interface is indistinct. In the upper valley, the lower layer is a lacustrine deposit consisting of silt/clay. The primary aquifers appear to be the alluvium in the upper basin and the Bouse in the lower basin. The water table (groundwater head) is typically found in alluvial sediments throughout the basin. Shrubs and other specialized desert plants are most abundant on the valley floor, associated with alluvial fans and washes (Figure 2).

2.2. In-situ measurements

Besides five regular meteorological stations in the basin, two new stations have been installed recently with soil moisture probes. These include two Soil Climate Analysis Network (SCAN) stations near Desert Center and Ford Dry Lake (Figure 1b). Data have been collected at depths of 5, 10, 20 and 50 cm below ground surface (bgs) at the SCAN stations since late 2011. A monitoring well, CWV1, was completed in 2012 to 300 m bgs near the outflow of the basin to collect groundwater and geophysical data in separate aquifer intervals, including natural gamma, electric resistivity, and sonic logs (Everett 2013). Using a linear sonic transit time formulation

corrected by gamma-log-based clay fraction data (RMC 1990), porosity was calculated at different depths of the well.

Well records from USGS Groundwater Watch, California Department of Water Resources (CADWR), and historical well logs were compiled by the Bureau of Land Management (BLM). We extracted well readings for calibration of the groundwater flow model. Some of these wells have estimates of transmissivity and conductivity derived from specific capacity and pumping tests records, which were also utilized.

2.3. Surface-subsurface processes modeling

2.3.1 PAWS+CLM model and default set up

The Process-based Adaptive Watershed Simulator coupled to the Community Land Model (PAWS+CLM) is a comprehensive and computationally-efficient model representing the whole-land phase of the hydrologic cycle (Shen *et al* 2016, 2014, 2013, Shen and Phanikumar 2010, Niu *et al* 2014) and reactive transport (Niu and Phanikumar 2015). The 2D unconfined aquifer receives recharge from 1D Richards' Equation-governed soil water flow and interacts with the quasi-3D saturated flow in confined aquifers below (Figure 3 caption). The model simulates percolation from washes over a smaller interface area using a leakance concept.

Prior to this study, PAWS were verified to match analytical solutions and was compared to other full-3D models (Maxwell *et al* 2014). In addition, PAWS+CLM satisfactorily reproduced a wide variety of field observations including streamflow, groundwater depths, leaf area index, evapotranspiration, soil moisture and temperature and water storage. PAWS+CLM can be deployed globally using available forcings and inputs (Riley and Shen 2014, Pau *et al* 2016, Ji *et al* 2015).

153 *2.3.2 Input to the numerical models*

154 For domain discretization, we use an 800 x 800 m^2 horizontal grid. 40 vertical layers, which are
155 exponentially finer near the surface, span the space between the ground surface and confined
156 aquifer. As described in *Shen et al.* (2014), we incorporated national 30 m digital elevation
157 model, landuse data, soils data (the desert sand category is later replaced with calibrated soil
158 parameters), and data from nationally-maintained weather stations in conjunction with our *in-situ*
159 meteorological stations. We fitted a linear model to the sonic-porosity data to set porosity (θ_s) as
160 a function of depth.

161 Two layers of aquifers are represented in PAWS+CLM. We used a gravity-data-derived bedrock
162 topography model to determine the bottom depth of the lower (Bouse/Fanglomerate/Clay) layer
163 (i.e., top of bedrock; Figure 4). A buried ridge, shown in Figure 4, is set as the western boundary
164 of the Bouse Formation. In the lower basin, we assumed a constant elevation for the top of the
165 second layer, since, as a marine/estuarine formation, the Bouse is observed to be flat. In the
166 upper valley, as there is no clear divide between formations nor detailed data coverage, a
167 constant thickness of ~90 m from geophysical surveys along a transect describes the sandy layer
168 above the lake deposit layer.

169 For the impervious mountains, soil thickness is set to 0.3 m, which is an average of depths found
170 during field reconnaissance. On the mountains, lateral groundwater flow can occur within this
171 thickness but may not percolate below. Mountain front subsurface recharge (Q_{MSub}) is recorded
172 as lateral subsurface flow that passes from thin mountain soil to the aquifer at the mountain foot.

173 *2.3.3 Soil parameter adjustment*

Soil parameters, including vertical conductivity, K_S, and van Genuchten parameters α and n, were adjusted on a trial and error basis for the alluvium and playa deposits based on *in-situ* moisture measurements. We tried to match not only the moisture peaks but also inter-peak minima. After suitable adjustment factors (multipliers and additions) had been found, we applied the parameters to their respective soil regimes.

2.4. Calibration of groundwater conductivity using MODFLOW+PEST

Although PAWS+CLM already contains a groundwater model, calibrating the spatial K field requires the MODFLOW+PEST package (Doherty 2003, Tonkin and Doherty 2009). A 2-layer MODFLOW model of the Chuckwalla Basin was set up for the valley portion of the basin.

In PAWS+CLM, there are three possible recharge sources: run-on infiltration in the washes, mountain-front subsurface flow, and direct soil column recharge. The long period (many years) required for recharge to reach the water table is a major practical obstacle. Therefore, we recorded the flux that travels downward through each cell interface five meters bgs. The flux that passes below this interface was regarded as the recharge that eventually reaches the water table. While at local scales there may be (discontinuous) clay layers that impede vertical flow, we are concerned with large-scale, long-term-average fluxes. We also added Q_{MSub} to the recharge. Time-averaged recharge was provided to the MODFLOW model, which has identical horizontal grid spacing as the PAWS+CLM model. MODFLOW+PEST was used to calibrate the K fields to water-table levels in observation wells. Constraining the possible range of K is important for reducing overfitting, where K is adjusted unrealistically to fit the noise rather than true signal. For the top aquifer layer, we added pumping-test-estimated K as known values and constrained K between [0.1-30] m/day. For the second layer, as pumping tests are rarer and most K estimates

196 are close to 1.5-4 m/day, we constrained the conductivity to [0.1-6] m/day. We used a warm-up
197 period of 4 years before extracting recharge.

198 *2.4.1 Groundwater withdrawals and boundary conditions*

199 Presently, a prison and a resort pump about 7100 m^3/day (2100 afy) and 3684 m^3/day (1090 afy)
200 from the Bouse and the alluvium formation, respectively (WorleyParsons 2010) (Figure 1).
201 These sink terms have existed for over two decades, and they have been included for calibrating
202 the steady-state model. For future projections, we added approved solar plants and the proposed
203 EMPS Project, as in Table 2, with water use values from their respective project EIA reports.

204 The Eastern boundary of the MODFLOW model ends at the western perimeter of the Palo Verde
205 Mesa agricultural zone, where USGS well data is available to build a fixed head boundary
206 condition to avoid modeling irrigation and withdrawals (Figure 1a). Mountain boundaries of the
207 MODFLOW model are set as no-flow boundary conditions, but as discussed earlier, mountain-
208 front subsurface inflow is added as recharge. The Pinto Basin connects to the Chuckwalla Basin
209 through a thin sedimentary neck (Figure 1a). No groundwater observations in the Pinto Valley
210 were readily available, so we used an average K value there in PAWS+CLM and excluded it
211 from calibration to reduce the number of parameters and overfitting. Simulated inflow from
212 Pinto is added as a source term to the Chuckwalla basin.

213 **2.5. Ensemble simulations, model rejection, and the dual-model approach**

214 Our goal of assembling an ensemble of simulations is not to estimate the probability distribution
215 of withdrawal impacts, but to put bounds on such impacts given large parametric uncertainties.
216 We first identified several key uncertain soil parameters (Table 3) for which preliminary
217 experiments showed strong impacts on recharge. We also tested a parameter describing

vegetation interception of runoff, but it was not found to be a sensitive parameter, likely because most recharge runs off from barren mountains. Then we perturbed the parameters simultaneously using global multipliers to generate recharges from high to low (Figure 5). Higher recharges lower the impact of pumping. The calibrated soil parameters served as the base case (#6) in these experiments.

After a recharge field was obtained, it was sent as input to the steady-state MODFLOW-PEST to calibrate K. We rejected a recharge if the calibrated head differed significantly from observed head despite the calibration, assessed using a z-test of the mean. To be lenient, we use 4 times of the residual variance from the best-calibrated case, $4 \cdot var_{min}$, for the z-test. We conducted chi-squared test on the residual variance and regression test with elevation as a predictor. If residuals are correlated to elevation, there is a regional pattern to the error which suggest the model/recharge is flawed. Furthermore, when the calibration overfits to data, it tends to force local K adjustment leading to large small-scale variations. To detect overfitting, we fitted a bi-quadratic surface to the K field, and calculate the standard deviation for the K residual from the surface. Five calibrations were conducted for each recharge case shown in Table 3, using different initial guesses of K.

Steady-state calibrations do not constrain storage parameters. For transient simulations, plausible ranges of the specific yield of the alluvium (S_y) and the specific storage of the lower layer (S_s) were considered in future projection runs. Three values were tested for S_y: [0.05, 0.10, 0.15]. A small value of 0.05 was estimated for Desert Center (WorleyParsons 2009). However, other estimates place the value around 0.15. For S_s, earlier studies for aquifers in this area have

bounded the range from $5*e^{-6}$ to $1*e^{-4}$, so three values were tested in this study: [$1*10^{-6}$, $5*10^{-6}$, $5*10^{-5}$].

3. Results

3.1. Soil moisture comparisons

After soil parameters are adjusted, the Richards'-Equation-based PAWS+CLM model was able to match the soil-moisture time series at both stations (Figure 6). The calibrated K_S values are around 0.1 m/day at both sites (Table 1), which is lower than the expected range for sandy soils. This value is in the low range of the values reported for Mojave Desert soils, which was measured between 0.07 to 350 m/day for old and young soils, respectively (Young *et al* 2004). However, despite some large rainfall events, the observed moisture seldom gets above 0.15, and spends the majority of the time below 0.05 (Figure 6). Therefore, the nonlinear unsaturated conductivity in the dry range, which can be orders of magnitude lower than K_S, plays a more important role in infiltration than K_S. The van Genuchten parameters are more influential than K_S for estimating infiltration and recharge, and might compensate for uncertainties in K_S.

3.2. Assessing and rejecting perturbed simulations

Five of the recharge fields, which are near either the high end or the low end of recharge rates from the experiments, were completely rejected due to their inability to fit the groundwater head (Tables 4 & 5). Figure 7 presents the observed vs calibration groundwater head for some examples of accepted and rejected simulations. Experiments #1 through #5, rejected by all tests, over-estimate the groundwater head (Tables 5), suggesting their recharge rates are too large. On the contrary, experiment #12 under-estimates groundwater head regardless of calibration, suggesting its recharge rate is too low. The ***z-test*** alone was able to rule out most of the cases from recharges 1-5 & 11-12. The elevation-regression test and detrended K variation by

262 themselves rejected some cases for recharges #6-#10. The variance test by itself did not reject
263 any cases. One calibration using recharge 11 was considered a borderline case.

264 Using recharge generated by the default parameter set above, the spatially-distributed hydraulic
265 head compares well with the observations (Figure 7), and the resulting K field is smooth. Overall
266 the magnitude and variation of K conform to our knowledge of the area. In addition, the
267 simulated groundwater contour (Figure 8) is in agreement with trends shown in earlier studies
268 (WorleyParsons 2010).

269 **3.3. Water balance of the basin under uncertainty**

270 The lower bound estimate of total inflow is 3.07 mm/yr, between #10 and #11 (7,107 afy, see
271 Table 4 caption). The upper bound of our inflow estimate is 4.99 mm/yr (11,564 afy), the
272 average between #5 and #6. Our estimates range from 3.4% to 5.6% of precipitation. In the
273 literature, recharge estimates in arid and semi-arid basins in the southern Mojave range from 3%-
274 7% of precipitation (Stonestrom *et al* 2007). Reports in nearby basins range from 2.8%-5.2%
275 (Whitt and Jonker in CGB 2004), down to 1.1% (Nishikawa *et al* 2005). Simulated recharge is
276 focused on ephemeral washes and alluvial fan on mountain fringes (Figure 9a). As runoff
277 reaches the alluvial fans, the thick sediment provides more volume for storage and infiltration.

278 The proposed withdrawal during the initial-fill phase of the EMPS Project (13,140 afy, from
279 Table 2), is larger than the upper bound of the recharge estimate. Even if we assume there is no
280 outflow to the Mesa Verde Valley, for the purpose of estimating maximum renewable extraction,
281 groundwater storage will likely decline significantly during the initial-fill stage. If the initial fill
282 is evenly distributed into 20 years, the annualized pumping is still more than the lower bound

283 estimate. Therefore, the system may be nearing, if not exceeding, its full sustainable groundwater
284 production capacity after the EMPS initiates.

285 **3.4. Projections of the impacts of pumping on groundwater sustainability**

286 Recharges from the retained simulations and their respective calibrated K fields were used to
287 estimate drawdown in response to new solar plant groundwater pumping. At EMPS, the largest
288 drawdown occurs at the end of the initial fill period and has a range of 8 to 11 meters when $S_y =$
289 0.05 (Figures 10a and 11). Without rejection of overfitted simulated recharge rates, this range
290 would have been 7 to 15.3 meters. The reduction of uncertainty depends on the site, as Desert
291 Sunlight sees a large reduction (Figures 10b) while Genesis almost sees no effect (Figures 10c).

292 For EMPS at $S_y = 0.05$, the drawdown reduces by 3~4 m within one year after the initial-fill
293 phase, then linearly declines over the next 16-year re-fill period. Heavy pumping induces a large
294 hydraulic gradient and a deep cone of depression. Once the pumping ceases, the large aquifer
295 transmissivity lead groundwater flow to rapidly fill the cone. The water table then gradually
296 declines during the project's re-fill phase. After the simulated cessation at the EMPS, the
297 drawdown can reduce by 4 m in one year, and at the end of simulation the water table recovers to
298 6-7 m from initial values. This pattern suggests that the system may be able to recover fast from
299 the assumed pumping, but the recovery speed does not imply it can go to pristine conditions. If
300 there is a boom of projects pumping groundwater, groundwater levels will not be sustainable, as
301 can be seen from the mass balance analysis. We also note the specific yield has larger impact
302 than recharge (Figures 11).

303 If, as in conventional methods, we had assumed a uniformly distributed recharge before
304 calibrating K, the results would have been much different, even with the same total recharge. The

305 uniform recharge tends to over-estimate head in the lower basin (Figure 12a). While the RMSE
306 is not very high, the resulting K fields have higher local variation. Also, the retained range of
307 pumping drawdown for the EMPS is larger (Figure 12c-f). However, such an effect is not
308 spatially homogeneous, as at the Genesis site uniform recharge leads to under-estimation of
309 pumping drawdown. This difference is because the EMPS Project is closer to mountain-front and
310 wash recharge. Since Genesis is located in the valley center and far from recharge locations, a
311 uniform recharge will over-estimate the recharge near the site. Therefore, the impacts of the
312 uniform-recharge assumption cannot be generically described.

313 **4. Discussion**

314 In the past, it has been difficult to simultaneously incorporate both soil moisture and spatially-
315 distributed groundwater data in modeling. The proposed dual-model approach appears effective
316 in identifying a plausible range of recharge for desert, mountainous regions. This framework is
317 also robust to some input errors. If there are recharge terms in a region that are omitted or over-
318 estimated, e.g., due to local clay impedance, ensemble members with perturbed parameters can
319 compensate for the error to some extent. Eventually, only roughly suitable recharges can pass the
320 test by groundwater observations. The calibrated K field significantly influences possible
321 drawdown and recovery, which is also why the integration of groundwater observations is
322 critically important.

323 Previous research on recharge in arid regions have heavily focused on infiltration beneath
324 washes. Our study suggests an overlooked area for potential recharge is alluvial fans. As
325 immediate recipients of mountain runoff, the fans and adjacent flat areas have the first chance to
326 hold and infiltrate water. While some chloride studies suggested little deep recharge under some
327 fans (Stonestrom *et al* 2004), other field (Houston 2002, Bull 1977) and modeling (Blainey and

Pelletier 2008, Munévar and Mariño 1999) studies found alluvial fans to be major recharge areas. The hydrologic processes may be highly local. Modeling results suggest there is a great need for relevant data, e.g., moisture or solute under the alluvial fans, to better quantify recharge and constrain modeling.

Water managers may find fast water table recovery to be re-assuring and use it as a guideline to manage water. However, as heavy pumping induces large hydraulic gradient. It is likely always followed by rapid recovery after cessation, even if pumping rates far exceed recharge and result in large storage loss. Therefore, the speed of recovery itself cannot indicate sustainability as the water may not recover to before-pumping levels.

This case is illustrative to solar development in the desert or water-scarce environment in the world, highlighting needs for technological advance and full-cycle resources accounting. A single pumped-storage project may use up all recharge in an area during its initial fill, raising questions about sustainability, water efficiency, and alternative technology. To adequately assess the cost, future life-cycle studies should examine the virtual groundwater (Marston *et al* 2015) embodied in the power produced and other commodities to comprehensively consider the best use of water resources.

5. Conclusion

We have proposed a novel, widely-applicable dual-model approach to providing a bounded estimate of the effects of new groundwater pumping for arid regions. The distributed hydrologic model can better approximate the locations and distributions of recharge, while incorporation of groundwater head data is crucial for constraining the recharge rates. Our results indicate conventional approaches of assuming uniform recharge will distort the calibrated K field and

yield very different projections. With limited data, we ascertain that groundwater levels will decrease across the basin over the life of the energy-storage Project. Once pumping ceases, groundwater levels may recover quickly but not to before-pumping levels. More of such projects will likely not be sustainable.

6. Acknowledgement

We appreciate Kristan Culbert and James Collins who have compiled information about wells and pumping test data. This paper does not represent the position of the United States government. The present work was partially developed within the framework of the Panta Rhei Research Initiative of the International Association of Hydrological Sciences (IAHS).

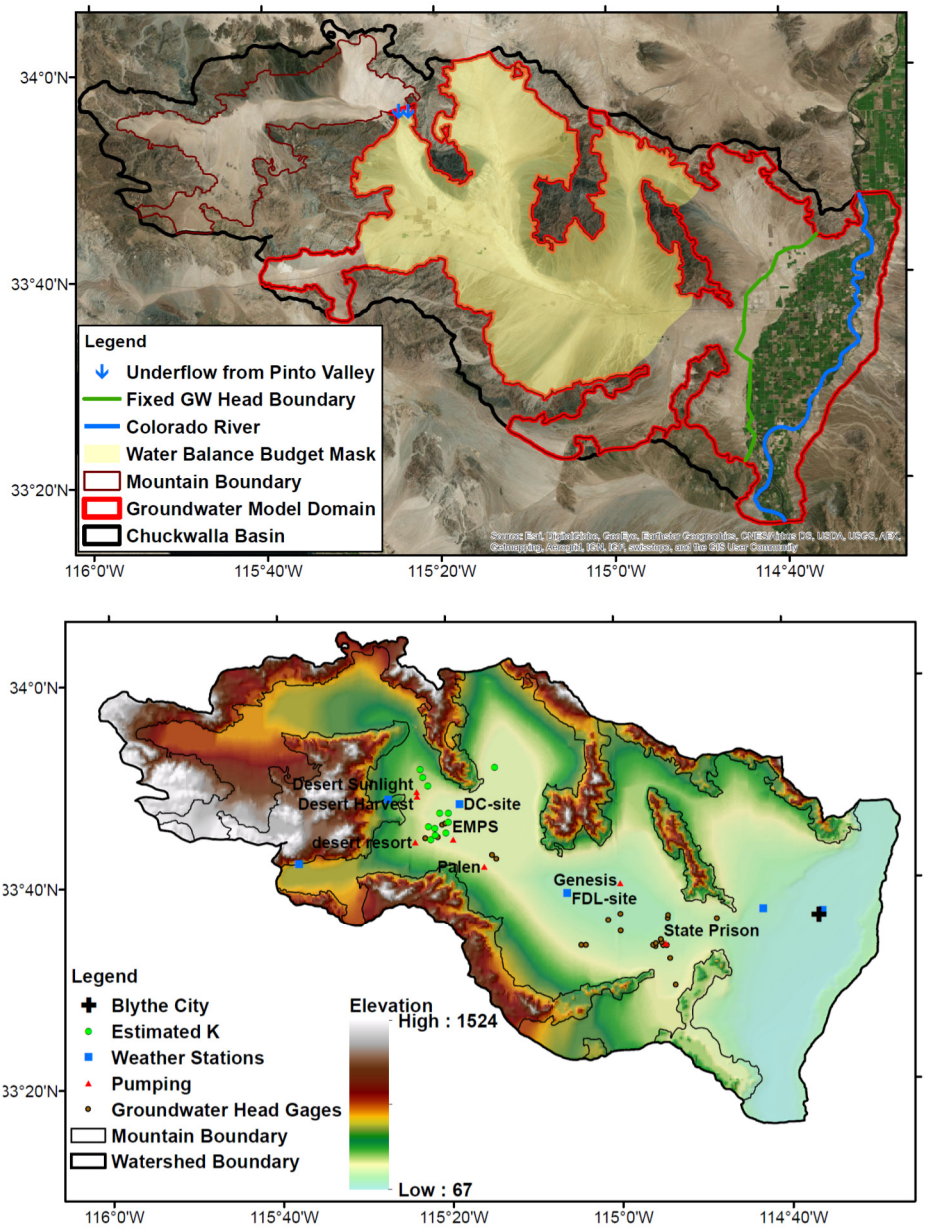

Figure 1. (a) Satellite image of the Chuckwalla basin and the modeling domain. The MODFLOW+PEST (Section 2.4) model domain is smaller than PAWS+CLM (Section 2.3.1) model domain. A fixed head boundary condition (green line), which was constructed by connecting known groundwater head, is set to encompass the agricultural region so that dynamics east to this line do not impact the calibration. The water balance budget mask refers to the area over which mass balance is reported. Fluxes are reported for this region because the agricultural region in the East and Pinto Valley in the Northwest are not included in the calibrated groundwater flow model; (b) map showing locations of observations, soil moisture stations including Ford Dry Lake (FDL) and Desert Center (DC), existing K estimates, existing pumping sources (the state prison and a desert resort), the solar plants (Palen, Desert Sunlight, Desert Harvest and Genesis) and Eagle Mountain Pumped Storage (EMPS) project.

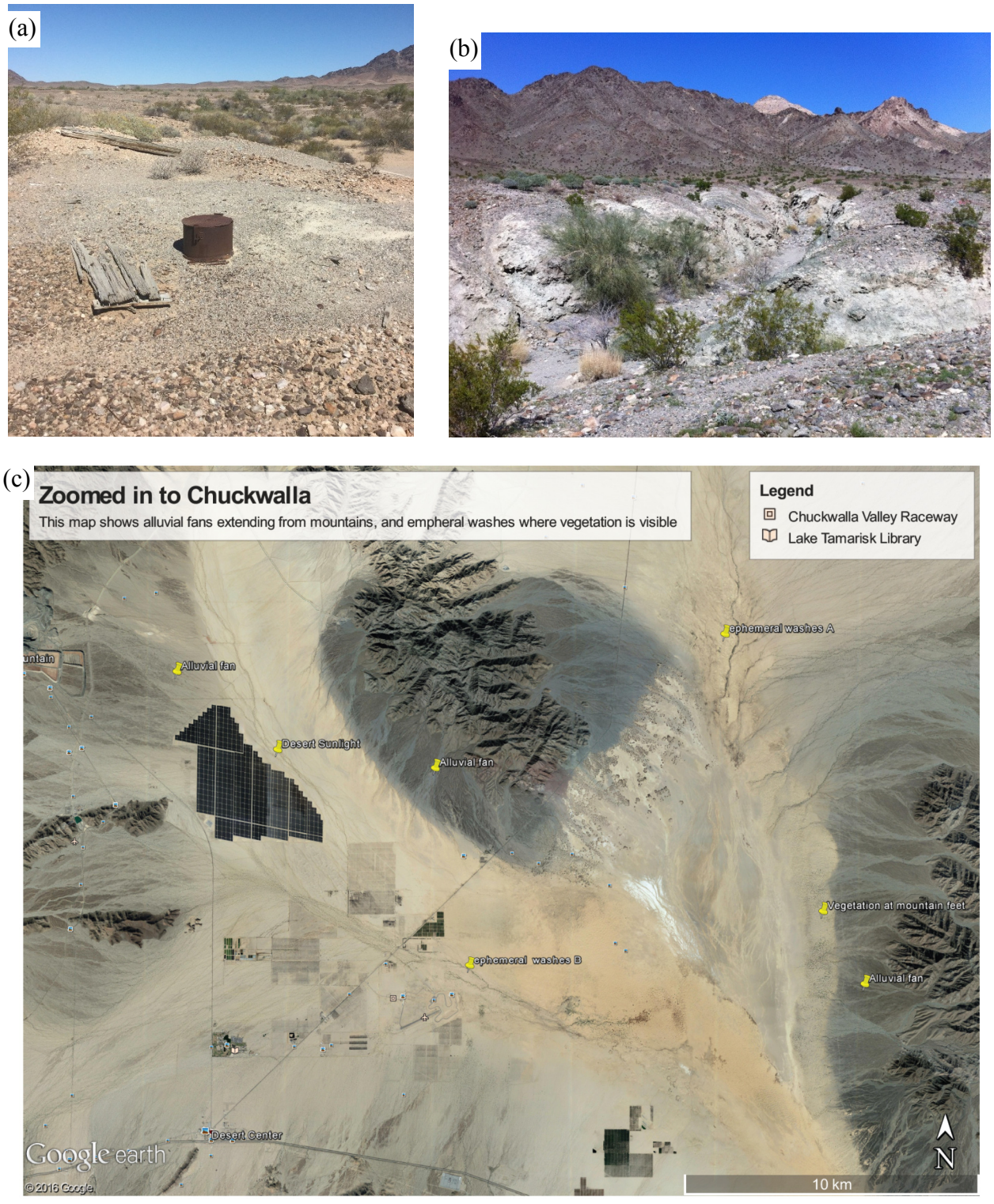

Figure 2. (a) A well in the basin surrounded by soils with visible desert pavement; (b) A picture taken within an alluvial fan looking upslope to higher elevations. Note that vegetation is visibly denser on the alluvial fan. Washes are also visible; (c) A zoomed-in satellite image of the Chuckwalla Valley, with annotated patterns of ephemeral washes and vegetation.

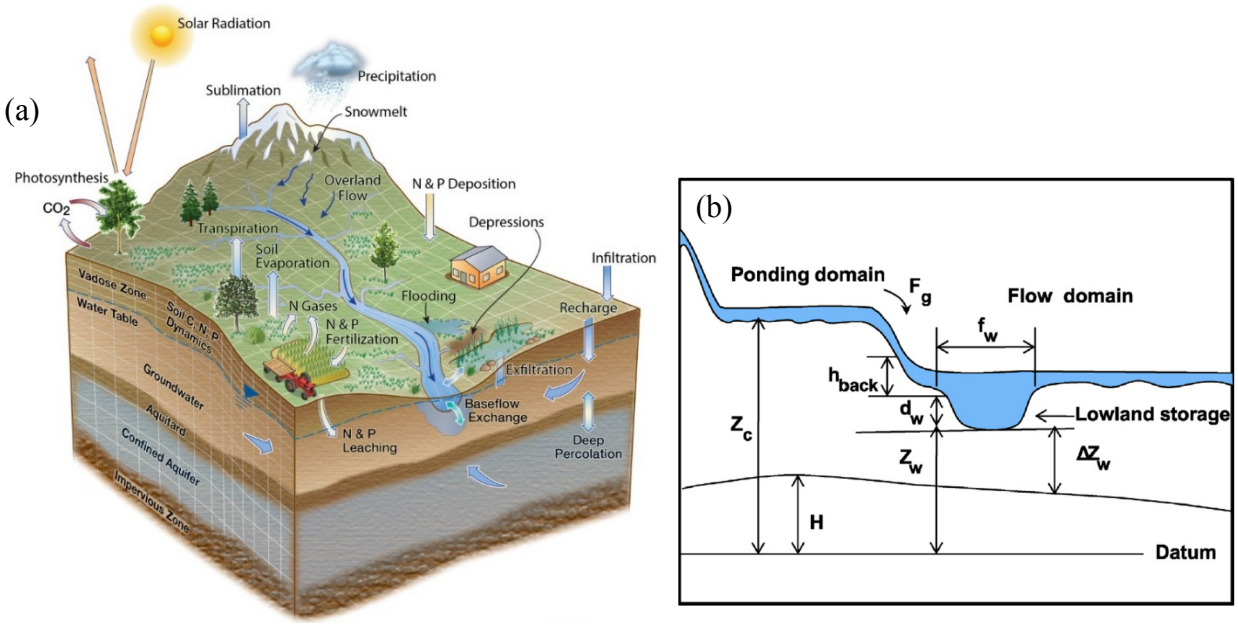

Figure 3. Sketch of PAWS+CLM hydrologic and ecosystem processes (reprinted from (Shen *et al* 2016) **with permission). Coupled vegetation photosynthesis, evapotranspiration, energy, carbon, and nitrogen cycles are provided by CLM, while hydrologic processes include soil water, groundwater, surface water and multi-way exchanges are provided by PAWS; (b) multi-way exchange between the flow domain, ponding domain, soil water and groundwater (reprinted from** (Shen *et al* 2013) **with permission): Surface water is divided into the flow domain, which can circulate laterally, and the ponding domain, which is connected to the soil matrix. The ponding domain contributes runoff to the flow domain while the latter may inundate the former during heavy flows. The flow domain is concentrated in a fraction of the cell termed f_w, following a micro-topographic parameterization in CLM4.5 (Oleson et al 2013). Flow domain water can evaporate at a potential rate as calculated by f_w multiplied by the Penman-Monteith equation. It can also percolate through the wash bed which will eventually reach the groundwater using the leakance concept** (Gunduz and Aral 2005)**.**

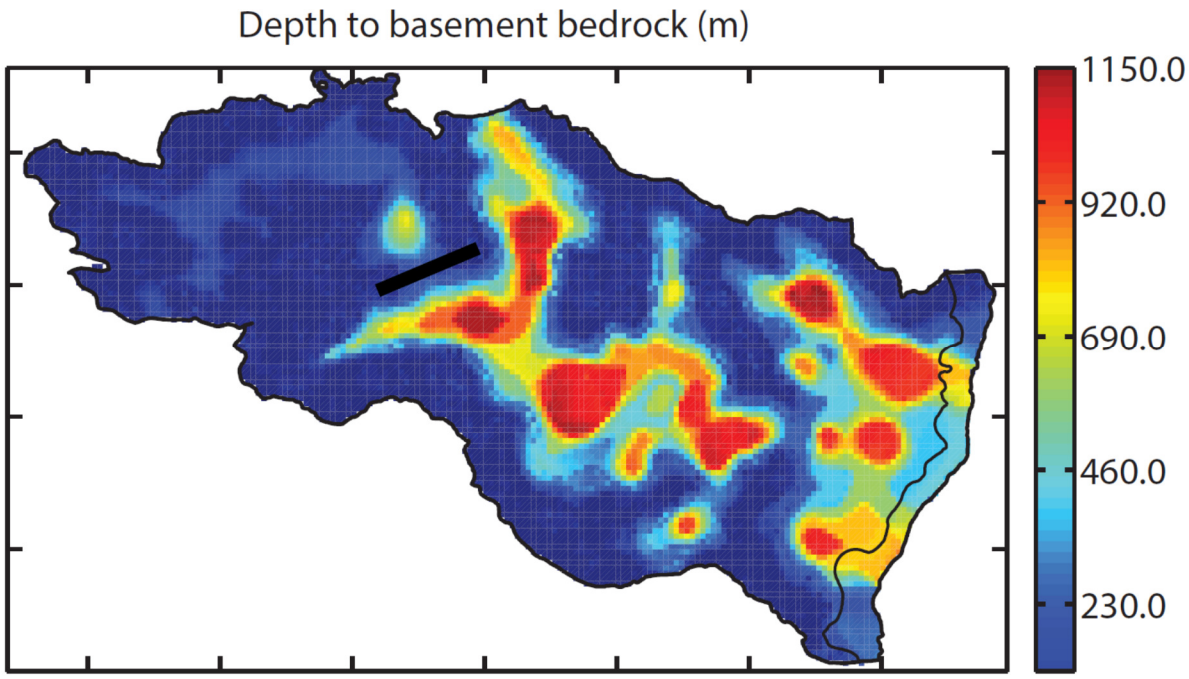

Figure 4. Depth to the basement bedrock map. The black thick line indicates a buried ridge that is visible in Figure 6 of Appendix C in (GEI 2010) **and multiple well-based transect profiles. In the lower valley, the bottom of the Bouse/Fanglomerate layer in the lower basin is available through gravity modeling. This model was constructed using Bouguer gravity data (Mariano *et al* 1986) and calibrated to bedrock depth measured from wells reaching the bedrock (Appendix 1 in (WorleyParsons 2009)). North to the buried ridge, Bouguer gravity data is also available from GeoPentech, which was reproduced in Figure 6 of Appendix C in (GEI 2010).**

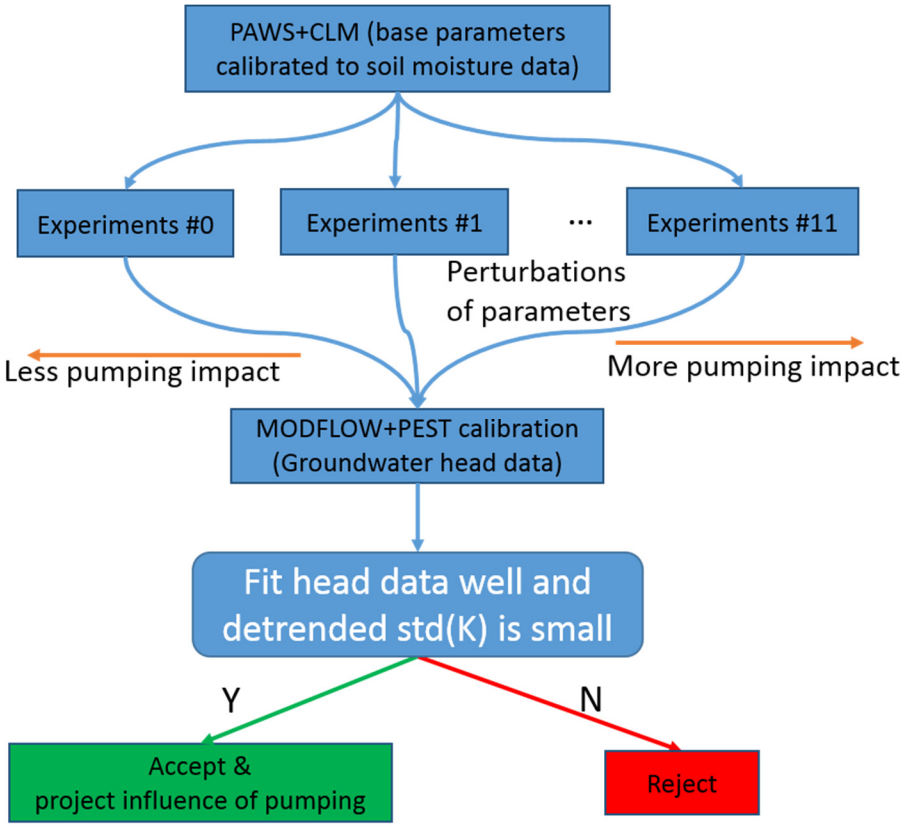

Figure 5. The proposed dual-model approach. We collected 4 years of field soil moisture measurements to estimate base soil properties. We then generated a range of recharge estimates by making perturbations to the calibrated soil parameters. Groundwater observations are used to constrain K in MODFLOW+PEST and, more importantly, retain or reject some of the recharge estimates. The retained recharges were used to produce the range of possible drawdowns induced by solar plant pumping, given the available information.

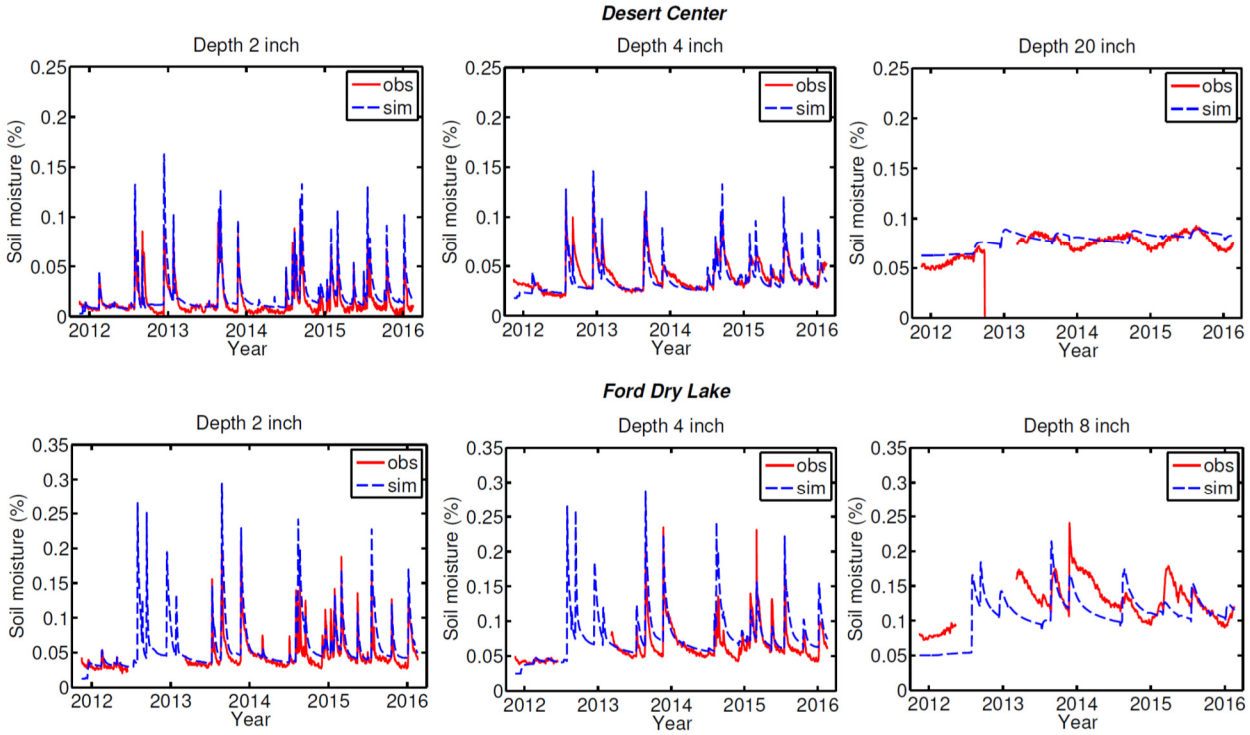

Figure 6. Soil moisture comparisons at the Desert Center site (upper three panels) and the Ford Dry Lake site (lower three panels). At the Desert Center site, the 8-inch probe appears to malfunction as it records moisture rises that are much larger than those detected at the surface. At 20-in depth, while the timing of the moisture wave is not completely correct, the amplitude of seasonal fluctuation is similar between observed and simulated.

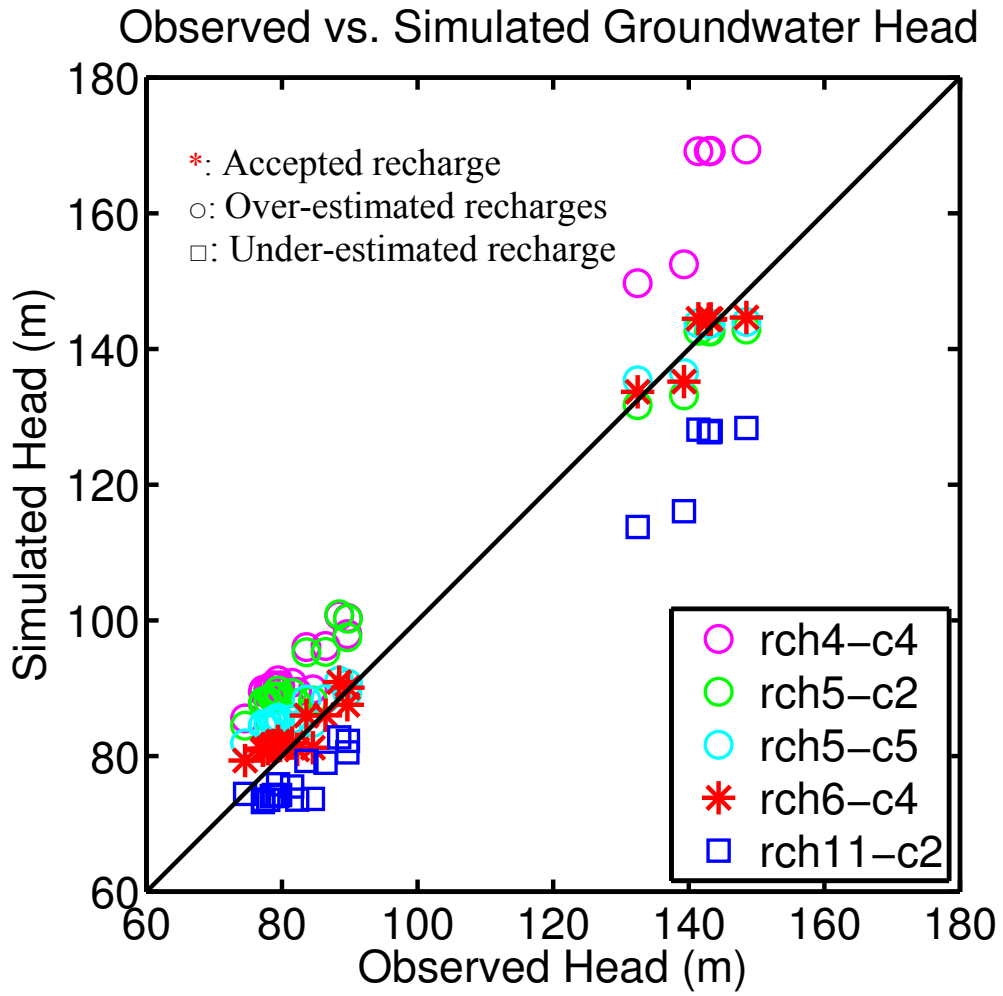

Figure 7. Observed vs. calibrated groundwater head for several recharges. "rch6-c3" means the calibration realization 3 (with a particular initial guess for K) using recharge from simulation #6. Other data series are defined similarly. We can see that with recharge #6 the calibrated head matches very well with the observed after calibration, with only a few meters of differences at the maximum for each data point. However, for recharge #4, the groundwater head is always over-estimated, regardless of the calibration effort and the initial guesses for K. Recharge #5 also tend to slightly over-estimate head in the lower basin (around observed head = 80 m). While the over-estimation is reduced in some calibration runs (rch5-c5), the K field tends to be overfitted. Recharge #11, on the other hand, is apparently under-estimated.

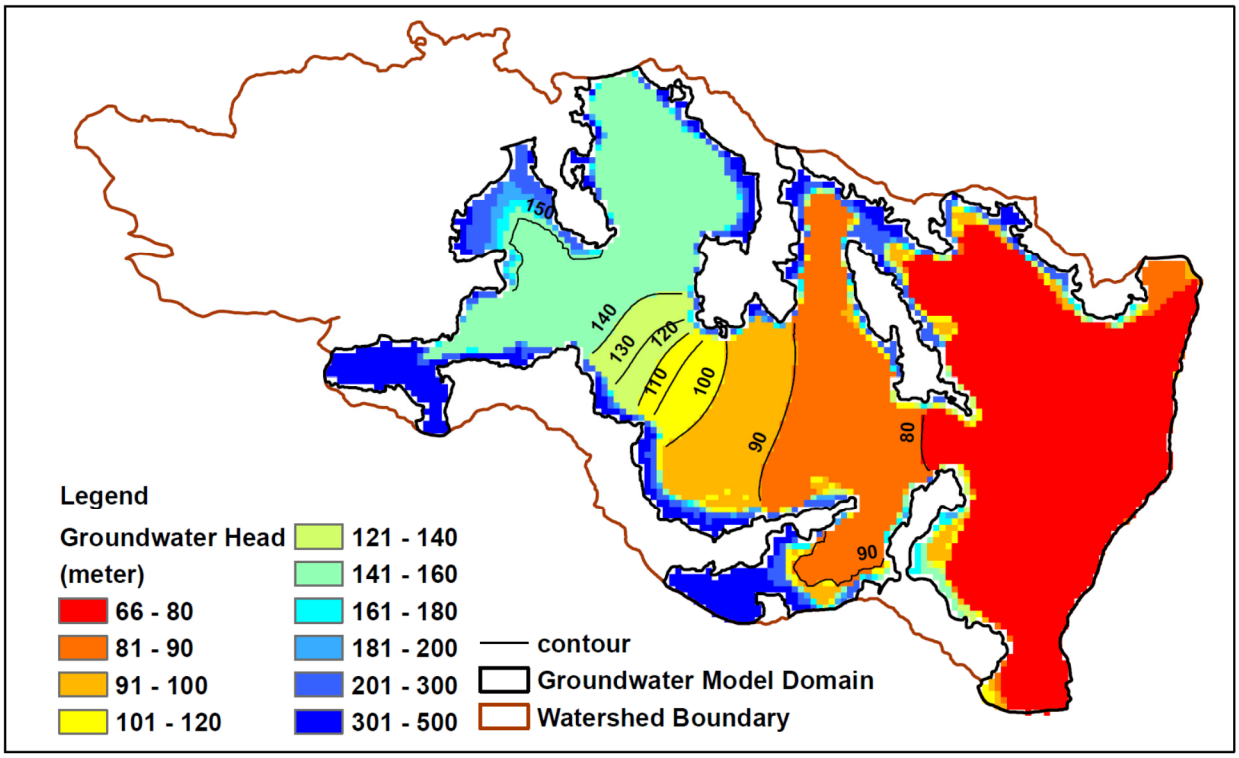

Figure 8. Simulated groundwater head map. This map does not include the effects of the assumed solar plant pumping. The Palo Verde Mesa Valley groundwater basin near Blythe (to the East of the mountain mouth) is controlled by the fixed head boundary condition.

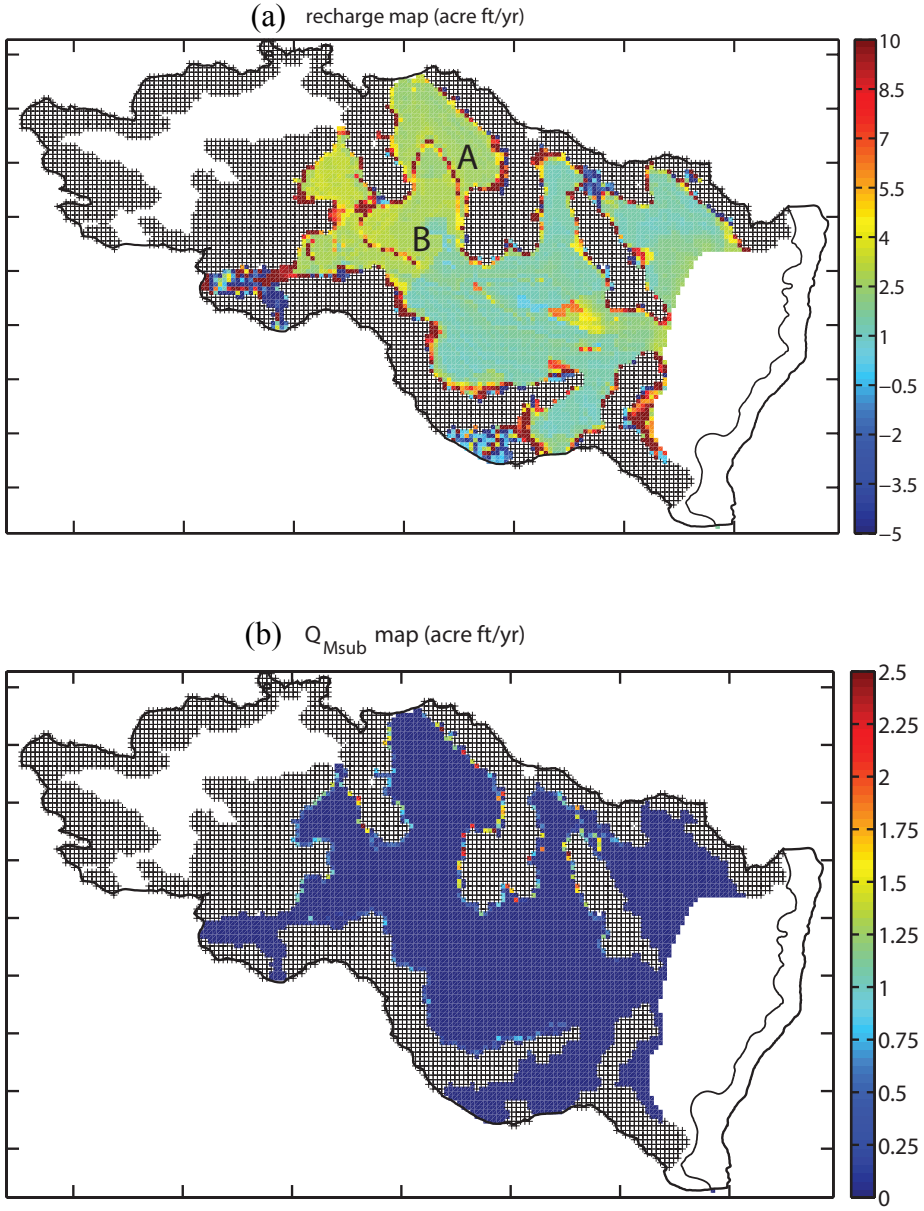

Figure 9. Simulated recharge maps from the base parameter set (experiment #6) (a) The total recharge, consisting of run-on percolation, soil matrix recharge, and mountain front subsurface recharge (Q_{MSub}). Note the percolation through flow paths along washes in annotated regions A and B, which agree with the vegetation pattern seen from Satellite images in Figure 2. Recharge also occurs at the alluvium that is the at the feet of mountains; (b) mountain-front subsurface recharge, which is lateral subsurface flow from thin mountain soils. Note that Q_{MSub} only occurs at the interface between mountain and valley. The cross hatched areas are the bedrock / mountain exposures. The Palo Verde Mesa Basin / Colorado River Floodplain (white area in the east) are not considered in the calibration. The Pinto Valley (white area to the northwest) is outside of the groundwater modeling domain, however, groundwater inflow to the Chuckwalla Basin is considered.

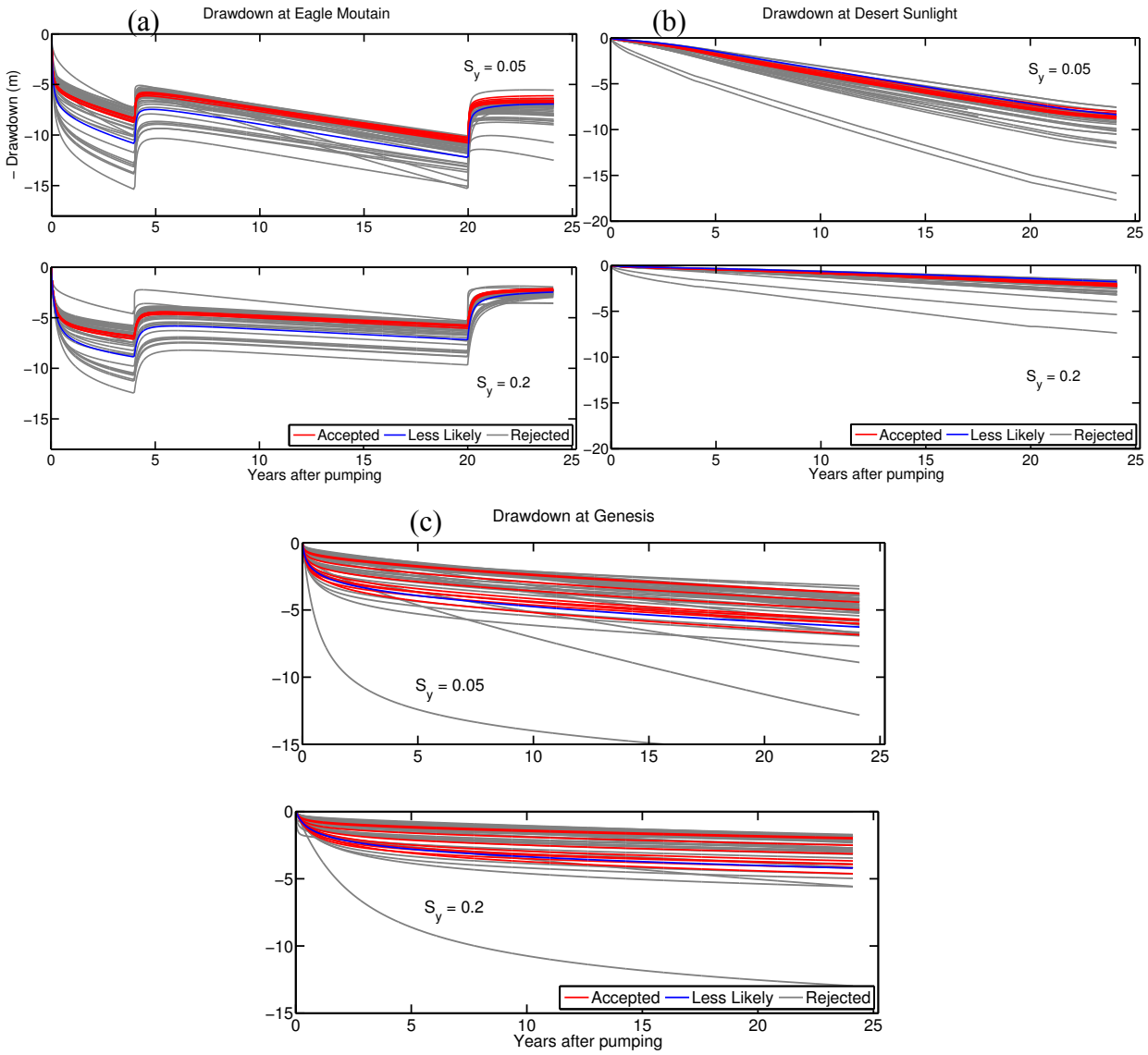

Figure 10 (a) Influence of assumed pumping on the water table at the Eagle Mountain Pumped Storage (EMPS) Project pumping site. The first 4 years is the initial fill phase. 5-20 years is the re-fill period. The pumping is terminated after 20 years to examine the rate of recovery. The red lines indicate accepted recharges. The magenta lines are "less-likely" recharges that have higher error statistically but could not be completely rejected. The drawdown is sensitive to the specific yield of the alluvium layer. It is not sensitive to the specific storage (S_s) in the range tested. The gray lines are the rejected recharges indicating the extent of uncertainty facing the prediction if no model rejection was applied. Note that the model rejection procedure reduces the uncertainty for EMPS. After 20 years of pumping, the maximum decline is likely around 35 ft for the case $S_y = 0.05$. (b) Same figure as in (a) but for the Desert Sunlight solar plant. The model rejection greatly reduces the uncertainty at this site; (c) the same Figure as (a) but for the Genesis solar plant. This site has more uncertainty than other pumping sites and the model rejection did not effectively reduce the uncertainty.

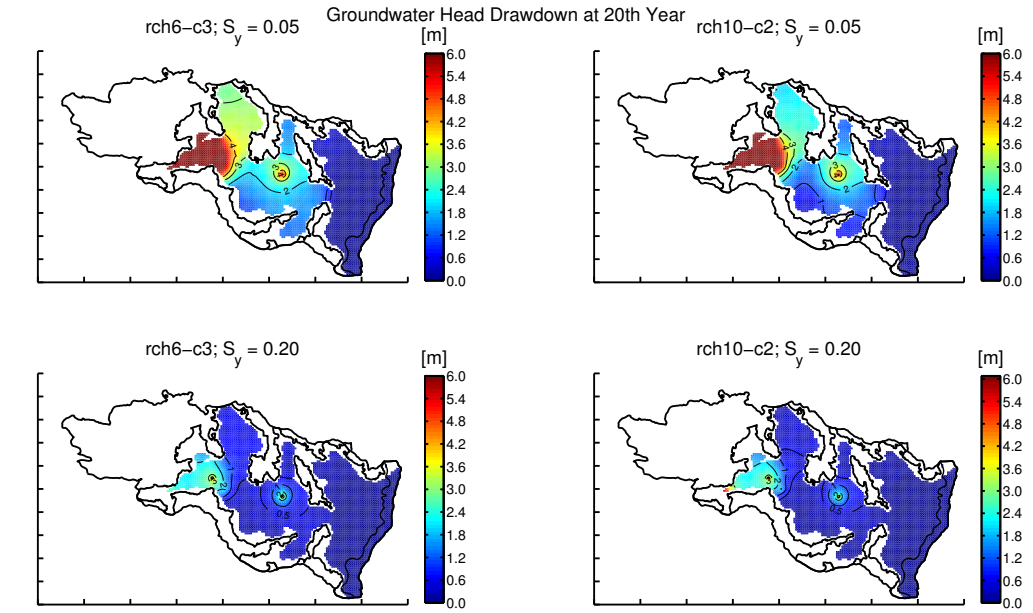

Upper 4 panels: Model layer 1

Lower 4 panels: Model layer 2

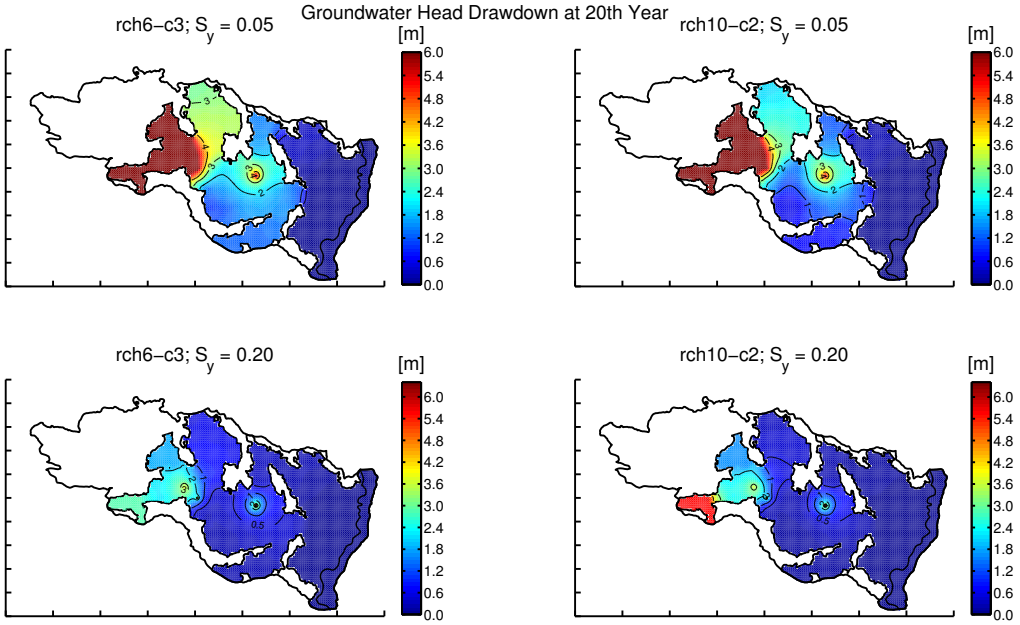

Figure 11. The cones of depression formed by the drawdowns (groundwater head from simulations without pumping minus that with pumping). To the west of Desert Center, the first model layer, with a thickness of ~50 ft, becomes dry after pumping. Rch6 is the highest accepted recharge while Rch10 is the lowest accepted recharge, which results in a deeper cone of depression. The drawdown is more sensitive to the assumption of S_y than the recharge employed.

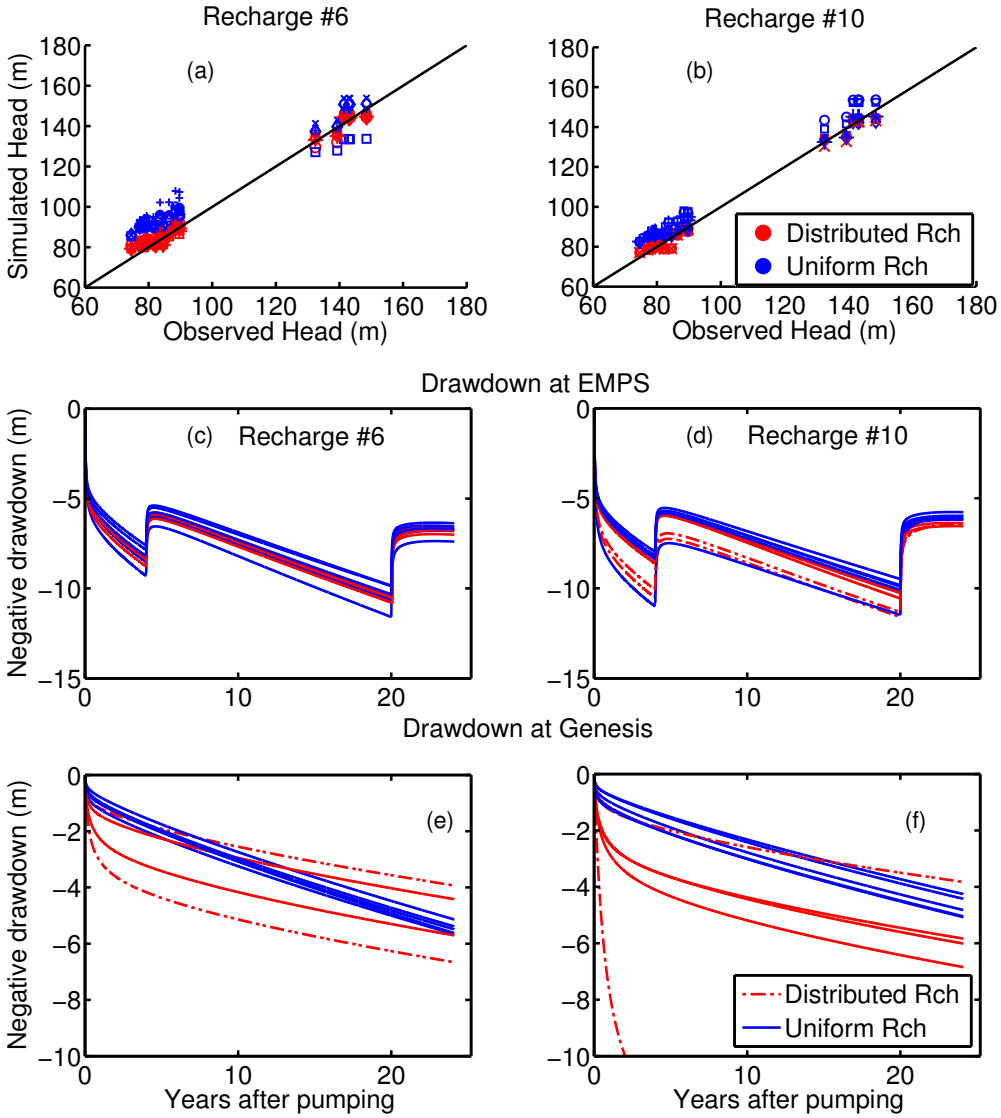

Figure 12. Comparing model-estimated recharge vs. uniform recharge for $S_y = 0.15$. No model rejection is applied to uniform-recharge simulations as they would have been rejected. Dashed lines indicated distributed-recharge simulations that have been rejected. (a-b) calibrated vs observed groundwater head: in the lower basin, uniform recharge tends to over-estimate groundwater head, which is due to under-estimating impacts of pumping; (c-f) projected impacts of pumping at EMPS and Genesis: uniform recharges produce a wider range of projected drawdown at EMPS but smaller range and less drawdown at Genesis. Not that the bottom 2 lines in the distributed-recharge case at Genesis have been rejected.

Table 1. Calibrated soil parameters on two field sites. Ks, N, α are kept constant throughout different depths. θ_r is adjusted at different depths to better fit the data. Note: the van Genuchten water retention formulation is written as $S = \frac{\theta(\psi)-\theta_r}{\theta_s-\theta_r} = (1 + |\alpha\psi|)^{-(N-1)/N}$, where S is relative saturation, ψ is the pressure head, θ is the moisture content, θ_r is the residual moisture content, θ_s is the saturated moisture content (porosity), and α and N are parameters. The unsaturated conductivity is calculated by $K_z(S) = K_S S^{\lambda}\left[1 - \left(1 - S^{N/(N-1)}\right)^{(N-1)/N}\right]^2$, where K_S is the saturated conductivity and $K_z(S)$ is the soil unsaturated vertical hydraulic conductivity at the relative saturation S.

Ford Dry Lake						
Depth	**Ks (m/day)**	**N (-)**	**α (m^{-1})**	**θ_r (-)**	**θ_s (-)**	**λ (-)**
2 in (layer 7)	0.1	1.6	4	0.00	0.3805	-1.2155
4 in (layer 9)	0.1	1.6	4	0.00	0.4221	-0.1059
8 in (layer 10)	0.1	1.6	4	0.02	0.4221	-0.1059
20 in (layer 12)	0.1	1.6	4	0.05	0.4221	-0.1059
Desert Center						
Depth	**Ks (m/day)**	**N (-)**	**α (m^{-1})**	**θ_r (-)**	**θ_s (-)**	**λ (-)**
2 in (layer 8)	0.12	1.8	3.2	1.00E-10	0.3877	-1.3
4 in (layer 11)	0.12	1.8	3.2	1.00E-10	0.3824	-1.3
8 in (layer 13)	0.12	1.8	3.2	0.025	0.3969	-1
20 in (layer 15)	0.12	1.8	3.2	0.06	0.3969	-0.8

Table 2. Pumping sources from the solar plants

	acre-ft-yr	x 10^3 m3/yr
Genesis	1525	1881
Desert Sunlight	52	64
Desert Harvest	53	65
Palen	220	271
Eagle Mountain (1-4 yrs)	8100	9992
Eagle Mountain (5-20 yrs)	1800	2220
Eagle Mountain (21-24 yrs)	0	0
Existing pumping	3190	3935
Total-- initial-fill (period 1, 1-4 yrs)	13140	16209
Total—re-supply (period 2, 5-20 yrs)	6840	8438
Total -- Decommissioned (period 3, 21-24 yrs)	5040	6217
20-year annualized total pumping	8100	9992

Table 3. Parameter perturbations for the numerical experiments. These changes are applied as multipliers or additions to default values. N/C means no change is applied. Going from Sim #1 to Sim #11, the resulting recharge decreases. Ks: vertical saturated soil conductivity; K: aquifer hydraulic conductivity; α and N are van Genuchten parameters as in Table 1 caption. K mostly influences Pinto underflow. Simulation #12 is derived from #11: it uses the same spatial distribution of recharge but multiplies the values by 0.8.

Parameter	Ks	α	K	K_S for mountain areas	Deep layer porosity for non-mountain areas	N
sim#1	× 10	× 1.5	× 3	N/C	× 1.2	N/C
sim #2	× 8	× 1.4	× 2.5	N/C	× 1	N/C
sim#3	× 6	× 1.3	× 2	N/C	× 1	N/C
sim#4	× 4	× 1.2	× 1.5	N/C	× 1	N/C
sim#5	× 2	× 1.1	× 1.25	N/C	× 1	N/C
sim#6	× 1	× 1	× 1	N/C	× 1	N/C
sim#7	× 1	× 1	× 1	=1.6 m/day	× 0.8	N/C
sim#8	× 0.75	× 0.85	× 0.5	N/C	× 0.7	N/C
sim#9	× 0.5	× 0.7	× 0.3	N/C	× 0.55	N/C
sim#10	× 0.5	× 0.7	× 0.3	=1.6	× 0.45	N/C
sim#11	× 0.5	× 0.7	× 0.3	N/C	× 0.55	-0.2
sim#12	× 0.5	× 0.7	× 0.3	N/C	× 0.55	-0.2

Table 4. Mass balance (in afy) and model acceptance status from the perturbed simulations. These fluxes are summed up for the "water balance budget mask" area in Figure 1a. 'mfront' means mountain-front subsurface recharge. A recharge is rejected is none of the 5 realizations was retained. Taking from #6, the upper bound of recharge is estimated as 11,564 afy. Because only one case from recharge #11 is narrowly retained, we take the average of the #10 and #11 to calculate the lower bound of recharge is estimated as 7,107 afy. Recharge #12 is the same simulation as #11, but the recharges are 80% of #11.

Recharge #	Soil & wash recharge	Pinto underflow	mfront	Total inflow	Prcp	Annualized pumping	Results
'sim#1'	18509	2236	298	21043	205,376	8101	Reject – always overestimate head
'sim#2'	18564	2335	316	21215	205,376	8101	Reject – always overestimate head
'sim#3'	16908	1777	241	18926	205,376	8101	Reject – always overestimate head
'sim#4'	15051	1212	223	16486	205,376	8101	Reject – always overestimate head
'sim#5'	12744	1012	225	13980	205,376	8101	Reject—either GW is over-estimated or K variation is too large
'sim#6'	10478	877	210	11564	205,376	8101	Accept 2 runs
'sim#7'	10594	825	182	11602	205,376	8101	Accept 1 run
'sim#8'	9487	522	173	10183	205,376	8101	Accept 1 run
'sim#9'	8539	372	136	9047	205,376	8101	Accept 3 runs
'sim#10'	7899	388	107	8394	205,376	8101	Accept 2 runs
'sim#11'	5309	320	191	5820	205,376	8101	Mostly rejected. One narrow retention retained as "unlikely"
'sim#12'	4247	320	191	4758	205,376	8101	Reject – always underestimate GW head

Table 5. Detailed metrics for model rejection. Green-filled cases pass all statistical tests. As shown in the legend, for every calibrated field (12 recharges, each with 5 calibration realizations), the numbers shown for each field are mean bias (upper left) of residuals (calibrated-observed head), root-mean-squared error (rmse, upper right), *p-value* for the elevation regression test (P_E, lower left), and standard deviation of the detrended K residuals (σ_K, lower right), respectively. To be lenient in retaining simulations, we implement relaxed rejection criteria for 3 statistical tests, using a confidence level of 2% and an assumed variance that is 4 times that of the best calibrated field (var_{min}, from recharge #10, realization 2). A field is rejected if one of the following is true for the calibrated head residuals: (a) the residuals fails the z-test for zero mean (upper left cell is then flagged red); (b) data rejects the null hypothesis that the residual variance is smaller than $4 \times var_{min}$ using a one-sided chi-squared test (upper right cell is then shallow blue); (c) the p-value for regressing residual to elevation (lower left cell is yellow); (d) $\sigma_K > 4.5$ (lower right is flagged dark blue). The hatched case, Rch#11 case 5, is a "border-line" case. It is the only retained case from Recharge #11 and it would have been rejected if, instead of 4, we had used 2.25 times var_{min}. Therefore we label it as "unlikely". We tried increasing soil conductivity on the mountains in simulation #7 but it was more often rejected.

Legend

bias	rmse
P_E	σ_K

	Realizations									
Recharge	*i*		*ii*		*iii*		*iv*		*v*	
1	13.4	14.0	5.6	13.5	11.4	12.8	35.7	36.4	6.9	13.2
	0.0%	6.1	0.0%	6.5	0.0%	7.4	0.0%	2.1	0.0%	8.1
2	86.9	87.1	49.9	51.4	5.9	13.9	45.5	51.2	12.2	13.6
	6.0%	1.3	0.0%	1.3	0.0%	6.6	0.0%	4.1	0.0%	7.8
3	34.6	36.3	4.4	11.0	34.6	36.3	8.9	10.6	8.9	10.6
	0.0%	6.8	0.0%	6.6	0.0%	2.3	0.0%	7.4	0.0%	7.4
4	1.1	11.0	5.2	7.3	1.7	10.4	14.0	15.4	7.1	7.9
	0.0%	6.1	0.0%	6.8	0.0%	6.0	0.6%	6.2	0.3%	6.8
5	11.3	15.3	6.1	8.2	4.5	5.9	6.2	18.9	3.1	4.5
	0.0%	1.3	0.0%	3.6	0.1%	3.7	0.0%	2.2	0.1%	6.8
6	2.0	3.8	1.1	2.7	1.1	2.6	1.1	2.6	1.0	2.6
	0.6%	3.9	20.4%	5.5	2.5%	4.6	8.6%	3.9	4.8%	4.3
7	4.5	5.1	6.7	7.6	1.1	2.6	-0.2	3.5	3.7	4.5
	92.4%	2.0	5.6%	2.2	5.2%	4.3	0.1%	4.5	17.7%	3.6
8	2.8	3.6	0.6	2.3	0.1	4.0	2.6	3.9	-0.3	3.1
	15.3%	2.6	21.7%	3.8	0.0%	5.3	0.1%	5.2	0.2%	5.1
9	0.2	2.2	1.9	3.1	0.4	2.3	1.8	3.2	0.2	2.3
	29.8%	3.9	1.2%	2.2	24.4%	3.4	2.7%	7.9	28.3%	4.1
10	0.1	2.2	0.1	2.2	3.8	5.4	-0.5	2.5	1.7	5.4
	13.4%	3.9	18.9%	2.1	13.3%	3.8	1.0%	4.0	2.4%	6.3
11	-11.5	14.6	-9.0	10.8	-11.7	15.1	-8.2	9.8	-1.6	4.5
	0.0%	4.1	0.0%	4.6	0.0%	5.7	0.1%	5.5	14.7%	3.8
12	-6.5	7.4	-11.1	13.3	-15.5	19.8	-6.4	7.0	-14.7	18.9
	15.2%	5.0	0.1%	3.5	0.0%	7.8	93.0%	4.4	0.0	6.9

548 **References**

549 Akbarzadeh A and Wadowski T 1996 Heat pipe-based cooling systems for photovoltaic cells
550 under concentrated solar radiation *Appl. Therm. Eng.* **16** 81–7 Online:
551 http://linkinghub.elsevier.com/retrieve/pii/1359431195000123

552 Alexandra Sims 2015 China builds huge solar power station which could power a million homes
553 *Indep. Environ.* Online: http://www.independent.co.uk/environment/china-builds-huge-
554 solar-power-station-which-could-power-a-million-homes-10446840.html

555 CADWR 1979 Sources of Powerplant Cooling Water in ttie Desert Area of Soutliern California
556 Reconnaissance Study *Calif. Dep. Water Resour. Bull. 91-24* Online:
557 http://www.water.ca.gov/waterdatalibrary/docs/historic/Bulletins/Bulletin_91/Bulletin_91-
558 24__1979.pdf

559 CGB 2004 Copper Mountain Valley Groundwater Basin *Calif. Groundw. Bull. 118* Online:
560 http://www.water.ca.gov/groundwater/bulletin118/basindescriptions/7-11.pdf

561 Doherty J 2003 Ground water model calibration using pilot points and regularization.
562 *Groundwater* **41** 170–7 Online: http://www.ncbi.nlm.nih.gov/pubmed/12656283

563 GEI 2010 Environmental Impact Analysis: Groundwater *Eagle Mt. Pumped Storage Proj. Draft*
564 *Environ. Impact Rep. Vol. I* Online:
565 http://www.waterboards.ca.gov/waterrights/water_issues/programs/water_quality_cert/eagle
566 mtn13123_eir.shtml

567 Gunduz O and Aral M M 2005 River networks and groundwater flow: a simultaneous solution of
568 a coupled system *J. Hydrol.* **301** 216–34 Online:
569 http://linkinghub.elsevier.com/retrieve/pii/S0022169404003269

570 Harbaugh A W 2005 *MODFLOW-2005, the U.S. Geological Survey modular ground-water*
571 *model -- the Ground-Water Flow Process: U.S. Geological Survey Techniques and Methods*
572 *6-A16.* (Reston, Virginia)

573 Homer C, Dewitz J, Yang L, Jin S, Danielson P, Xian G, Coulston J, Herold N, Megown J and
574 K. W 2015 Completion of the 2011 National Land Cover Database for the Conterminous
575 United States – Representing a Decade of Land Cover Change Information *Photogramm.*
576 *Eng. Remote Sensing* **81** 345–54

577 Ji X, Shen C and Riley W J 2015 Temporal evolution of soil moisture statistical fractal and
578 controls by soil texture and regional groundwater flow *Adv. Water Resour.* **86** 155–69
579 Online: http://www.sciencedirect.com/science/article/pii/S0309170815002341

580 Jokadar Z and Ponte C 2012 Specific Environmental and Social Impact Assessment Volume 1
581 *Ouarzazate Sol. Power Complex, Phase 1, Morocco.* Online:

http://www.masen.ma/media/uploads/documents/Masen_NOORoI_SESIA_Volume1_aDfethF.pdf

Mariano J, Helferty M G and Gage T 1986 Bouger and Isostatic Residual Gravity Maps of the Colorado River Region, including the Kingman, Needles, Salton Sea, and El Centro Quadrangles *Open-File Rep. 86-347* Online: https://pubs.er.usgs.gov/publication/ofr86347

Markstrom S L, Niswonger R G, Regan R S, Prudic D E and Barlow and P M 2008 GSFLOW—Coupled Ground-Water and Surface-Water Flow Model Based on the Integration of the Precipitation-Runoff Modeling System (PRMS) and the Modular Ground-Water Flow Model (MODFLOW-2005) *U.S. Geol. Surv. Chapter 1 Sect. D, Ground-Water/Surface-Water B. 6, Model. Tech.* Online: http://pubs.usgs.gov/tm/tm6d1/

Maurer D K and Berger D L 2006 Water Budgets and Potential Effects of Land- and Water-Use Changes for Carson Valley, Douglas County, Nevada, and Alpine County, California *USGS Sci. Investig. Rep. 2006–5305* Online: https://pubs.usgs.gov/sir/2006/5305/pdf/sir20065305.pdf

Maxey G B and Eakin T . 1949 Groundwater in the White River Valley, White Pine, Nye, and Lincoln counties, Nevada *Water Resour. Bull. No. 8, State Nevada, Off. State Eng.* Online: https://www.nrc.gov/docs/ML0331/ML033140348.pdf

Maxwell R M and Miller N L 2005 Development of a coupled land surface and groundwater model *J. Hydrometeorol.* **6** 233–47 Online: http://journals.ametsoc.org/doi/abs/10.1175/JHM422.1

Maxwell R M, Putti M, Meyerhoff S, Delfs J-O, Ferguson I M, Ivanov V, Kim J, Kolditz O, Kollet S J, Kumar M, Lopez S, Niu J, Paniconi C, Park Y-J, Phanikumar M S, Shen C, Sudicky E A and Sulis M 2014 Surface-subsurface model intercomparison: A first set of benchmark results to diagnose integrated hydrology and feedbacks *Water Resour. Res.* **50** 1531–49 Online: http://doi.wiley.com/10.1002/2013WR013725

McFadden L D, Wells S G and Jercinovich M J 1987 Influences of eolian and pedogenic processes on the origin and evolution of desert pavements *Geology* **15** 504 Online: http://geology.gsapubs.org/cgi/doi/10.1130/0091-7613(1987)15%3C504:IOEAPP%3E2.0.CO;2

McMichael C E, Hope A S and Loaiciga H A 2006 Distributed hydrological modelling in California semi-arid shrublands : MIKE SHE model calibration and uncertainty estimation *J. Hydrol.* **317** 307–24

Metzger D G, Loeltz O J and Irelna B 1973 *Geohydrology of the Parker-Blythe-Cibola Area, Arizona and California, United States Geological Survey Professional Paper 486-G* (Washington, D. C.)

Mirus B B, Perkins K S, Nimmo J R and Singha K 2009 Hydrologic Characterization of Desert Soils with Varying Degrees of Pedogenesis: 2. Inverse Modeling for Effective Properties *Vadose Zo. J.* **8** 496 Online: https://www.soils.org/publications/vzj/abstracts/8/2/496

Moharram K A, Abd-Elhady M S, Kandil H A and El-Sherif H 2013 Enhancing the performance of photovoltaic panels by water cooling *Ain Shams Eng. J.* **4** 869–77

NCDC 2014 National Climatic Data Center (NCDC): U.S. Daily Surface Data (COOP Daily/Summary of Day) Online: https://www.ncdc.noaa.gov/cdo-web/

NHD 2014 National Hydrography Dataset (NHD) *United States Geol. Surv.* Online: http://nhd.usgs.gov/

Nishikawa T, Izbicki J A, Hevesi J A and Martin C L S P 2005a Evaluation of Geohydrologic Framework, Recharge Estimates and Ground-Water Flow of the Joshua Tree Area, San Bernardino County, California *USGS Sci. Investig. Rep. 2004-5267* Online: https://pubs.usgs.gov/sir/2004/5267/

Nishikawa T, Izbicki J A, Hevesi J A and Martin C L S P 2005b Evaluation of Geohydrologic Framework, Recharge Estimates and Ground-Water Flow of the Joshua Tree Area, San Bernardino County, California *USGS Sci. Investig. Rep. 2004-5267*

Niu J and Phanikumar M S 2015 Modeling watershed-scale solute transport using an integrated, process-based hydrologic model with applications to cacterial fate and transport *J. Hydrol.* **529** 35–48 Online: http://www.sciencedirect.com/science/article/pii/S0022169415005089

Niu J, Shen C, Li S-G and Phanikumar M S 2014 Quantifying storage changes in regional Great Lakes watersheds using a coupled subsurface-land surface process model and GRACE, MODIS products *Water Resour. Res.* **50** 7359–77 Online: http://doi.wiley.com/10.1002/2014WR015589

NRCS 2010 SSURGO Soil Survey Geographic Database *Nat. Resour. Conserv. Serv.* Online: http://www.nrcs.usda.gov/wps/portal/nrcs/detail/soils/survey/?cid=nrcs142p2_053627

Oleson K W, Lawrence D M, Bonan G B, Drewniak B, Huang M, Koven C D, Levis S, Li F, Riley W J, Subin Z M, Swenson S C, Thornton P E, Bozbiyik A, Fisher R, Heald C L, Kluzek E, Lamarque J-F, Lawrence P J, Leung L R, Lipscomb W, Muszala S, Ricciuto D M, Sacks W, Sun Y, Tang J and Yang Z-L 2013 Technical Description of version 4.5 of the Community Land Model (CLM) *NCAR/TN-503+STR, NCAR Tech. Note* Online: http://www.cesm.ucar.edu/models/cesm1.2/clm/CLM45_Tech_Note.pdf

Owen-Joyce S J, Wilson R P, Carpenter M C and Fink J B 2000 Method to identify wells that yield water that will be replaced by water from the Colorado River downstream from

650 Laguna Dam in Arizona and California *Water-Resources Investig. Rep. 00-4085* Online:
651 http://pubs.usgs.gov/wri/2000/4085/report.pdf

652 Pau G S H, Shen C, Riley W J and Liu Y 2016 Accurate and efficient prediction of fine-
653 resolution hydrologic and carbon dynamic simulations from coarse-resolution models *Water*
654 *Resour. Res.* Online: http://doi.wiley.com/10.1002/2015WR017782

655 Rehman S, Al-Hadhrami L M and Alam M M 2015 Pumped hydro energy storage system: A
656 technological review *Renew. Sustain. Energy Rev.* **44** 586–98 Online:
657 http://www.sciencedirect.com/science/article/pii/S1364032115000106

658 Rigon R, Bertoldi G and Over T M 2006 GEOtop: A distributed hydrological model with
659 coupled water and energy budgets *J. Hydrometeorol.* **7** 371–88 Online:
660 http://journals.ametsoc.org/doi/abs/10.1175/JHM497.1

661 Riley W J and Shen C 2014 Characterizing coarse-resolution watershed soil moisture
662 heterogeneity using fine-scale simulations *Hydrol. Earth Syst. Sci.* **18** 2463–83 Online:
663 http://www.hydrol-earth-syst-sci.net/18/2463/2014/hess-18-2463-2014.html

664 SCAN 2017 Desert Center SCAN station *Soil Clim. Anal. Netw. Stn.* Online:
665 https://wcc.sc.egov.usda.gov/nwcc/site?sitenum=2183&state=CA

666 Shen C, Niu J and Fang K 2014 Quantifying the effects of data integration algorithms on the
667 outcomes of a subsurface–land surface processes model *Environ. Model. Softw.* **59** 146–61
668 Online: http://www.sciencedirect.com/science/article/pii/S1364815214001376

669 Shen C, Niu J and Phanikumar M S 2013 Evaluating controls on coupled hydrologic and
670 vegetation dynamics in a humid continental climate watershed using a subsurface - land
671 surface processes model *Water Resour. Res.* **49** 2552–2572 Online:
672 http://doi.wiley.com/10.1002/wrcr.20189

673 Shen C and Phanikumar M S 2010 A process-based, distributed hydrologic model based on a
674 large-scale method for surface–subsurface coupling *Adv. Water Resour.* **33** 1524–41 Online:
675 http://linkinghub.elsevier.com/retrieve/pii/S0309170810001569

676 Shen C, Riley W J, Smithgall K M, Melack J M and Fang K 2016 The fan of influence of
677 streams and channel feedbacks to simulated land surface water and carbon dynamics *Water*
678 *Resour. Res.* **52** 880–902

679 Stone P 2006 Geologic Map of the West Half of the Blythe 30’ by 60’ Quadrangle, Riverside
680 County, California and La Paz County, Arizona *USGS Sci. Investig. Map 2922* Online:
681 https://pubs.usgs.gov/sim/2006/2922/

682 Therrien R, McLaren R G, Sudicky E A and Panday S M 2006 HydroGeoSphere: A three-
683 dimensional numerical model describing fully-integrated subsurface and surface flow and
684 solute transport *Groundwwater Simul Gr. Waterloo Ont* 349

685 Tonkin M, Doherty J and Moore C 2007 Efficient nonlinear predictive error variance for highly
686 parameterized models *Water Resour. Res.* **43** 1–15

687 USGS 1995 Groundwater Atlas of the United States, California and Nevada *United States Geol.*
688 *Surv. Hydrol. Investig. Atlas HA-730-B* Online: http://pubs.usgs.gov/ha/ha730/ch_b/

689 Wilson J L and Guan H 2004 Mountain-Block Hydrology and Mountain-Front Recharge
690 *Groundwater Recharge in a Desert Environment: The Southwestern United States* Water
691 Science and Application vol 9, ed J F Hogan, F M Phillips and B R Scanlon (Washington,
692 D. C.: American Geophysical Union) Online: http://www.agu.org/books/ws/v009/

693 WorleyParsons 2010 Genesis Solar Energy Project Groundwater Resources Investigation *Rep. to*
694 *Calif. Energy Comm.* Online:
695 http://www.energy.ca.gov/sitingcases/genesis_solar//documents/applicant/2010-02-
696 11_Groundwater_Resources_Investigation_TN-55916.pdf

697 WorleyParsons 2009 Groundwater resources investigation, Genesis Solar Energy Project,
698 Riverside Country, California *Genes. Sol. Energy Proj. Appl. Certif. Vol. I* Online:
699 http://www.energy.ca.gov/sitingcases/genesis_solar/documents/applicant/afc/volume_1/

700 Wösten J H M, Pachepsky Y A and Rawls W J 2001 Pedotransfer functions: bridging the gap
701 between available basic soil data and missing soil hydraulic characteristics *J. Hydrol.* **251**
702 123–50 Online: http://linkinghub.elsevier.com/retrieve/pii/S0022169401004644

703 Young M, McDonald E, Caldwell T, Benner S and Meadows D 2004 Hydraulic Properties of a
704 Desert Soil Chronosequence in the Mojave Desert, USA *Vadose Zo. J.* **3** 956–63 Online:
705 http://scholarworks.boisestate.edu/geo_facpubs/133

706